Scientific Reports

https://doi.org/10.1038/s41598-026-42156-0

Article in Press

A stress-controlled reservoir formation model for ultra-deep sandstones in foreland thrust belts: case study of the cretaceous bashijiqike formation, bozi-dabei area, kuqa depression, tarim basin

Received: 24 January 2026

Accepted: 24 February 2026

Published online: 28 February 2026

Cite this article as: Wang C., Zhong D., Mo T. *et al.* A stress-controlled reservoir formation model for ultra-deep sandstones in foreland thrust belts: case study of the cretaceous bashijiqike formation, bozi-dabei area, kuqa depression, tarim basin. *Sci Rep* (2026). https://doi.org/10.1038/s41598-026-42156-0

Chenguang Wang, Dakang Zhong, Tao Mo & Haitao Sun

A Stress-Controlled Reservoir Formation Model for Ultra-Deep Sandstones in Foreland Thrust Belts: Case Study of the Cretaceous Bashijiqike Formation, Bozi-Dabei Area, Kuqa Depression, Tarim Basin

Chenguang Wang ,Dakang Zhong,Tao Mo,Haitao Sun

Wang Chenguang,wcgzhy123@163.com
Zhong Dakang,dakangzhong@263.Net
Mo Tao, mttlmoil@163.com
Sun Haitao,haitao.sun@cup.edu.cn

Abstract: The ultra-deep tight sandstone reservoirs of the Lower Cretaceous Bashijiqike Formation in the Kelasu Structural Belt, Kuqa Depression, have been significantly influenced by intense lateral tectonic compression since the late Himalayan period (ca. 5 Ma), resulting in the formation of fractured tight sandstone reservoirs. Deciphering the control of the stress-strain state on reservoir quality is crucial for establishing a predictive model. This study systematically investigates the impact of stress state and strain degree on reservoir quality through thin-section identification, analysis of rock mechanical parameters, triaxial stress tests, and rock stress-strain experiments on samples from typical structural positions. The results show that: (1) Sandstones in the hanging wall of the Kelasu Fault experienced weak tectonic compression, characterized by low paleo-stress and present-day stress, minimal strain, and relatively high porosity (10%–14%). (2) Footwall sandstones exhibit higher stress and strain than those in the hanging wall, with notable spatial variations: proximal footwall areas display low vertical stress due to thrusting from the hanging wall, forming collapse structures with weak compression, good physical properties (porosity ~10%), and underdeveloped fractures; distal footwall areas show concentrated stress accumulation and the strongest relative/effective compressive stress. These areas develop intensely compressed imbricated and pop-up structures with high strain, low porosity (<5%), and well-developed fractures. (3) The eastern Keshen area in the footwall has long been subjected to deep burial and intense compression, exhibiting higher strain, relatively lower porosity, and more developed fractures than the western Dabei and Bozi areas at similar structural positions. These findings

reveal how stress-strain variations, controlled by structural positioning, govern reservoir quality. This supports a new genetic model for reservoir formation in the Kelasu Structural Belt and provides key geological insights for reservoir prediction in future natural gas exploration and development.

Keywords: Ultra-deep tight sandstone; Kuqa Depression; Bashijiqike Formation; Geomechanics; Pore-fracture evolution; Reservoir heterogeneity

0 Introduction

Global deep and ultra-deep oil and gas resources are abundant. By the end of 2020, 2,111 deep oil and gas reservoirs had been discovered, 68 of which are buried at depths exceeding 8,000 meters. The increasing number of deep and ultra-deep reservoir layers discovered in basins demonstrates excellent exploration potential, establishing these depths as a crucial frontier for global oil and gas exploration and development [1-3]. In foreland compressional settings, while intergranular pores remain the primary pore type in most deep to ultra-deep clastic rocks, the role of fractures (including those enlarged by dissolution) is significant and should not be underestimated. At ultra-deep depths, these storage structure types are critically important for rock permeability [4-7].

Recent years have witnessed significant progress in the study of ultra-deep reservoirs under foreland compression. Multiple scholars have discovered that, under such compression, tectonic parallel shortening is primarily achieved through interlayer parallel compaction. When confining pressure and/or shear stress exceed a critical threshold, pore collapse leads to porosity loss, representing an irreversible deformation. This form of compressional failure in porous rocks is termed shear-enhanced compaction. In shallow layers, deformation bands are a typical manifestation of stress mode control on reservoirs. Fossen, considering factors such as deformation band mineralogy, grain size, grain shape, sorting, cementation degree, porosity, and stress state, classified deformation bands in sandstones into four categories based on formation mechanisms: disaggregation bands, phyllosilicate bands, cataclastic bands, and solution/cementation bands. Both disaggregation bands and fracture bands result from porosity change induced by typical stress modes. In deep to ultra-deep layers, the evolution model of high-quality pores is controlled by the tectonic compression style and

the stress state of specific structural positions. For instance, Edward A. et al. discovered that overpressure occurred in local structural positions during the compression of the Cusiana Field in the Llanos Foothills of Colombia, leading to porosity preservation. Simulations of multiple BTH collisions by Miyakawa indicated that porosity changes in the target layer initially decreased due to lateral compression but later gradually increased due to minor uplift and fracture formation [8-11].

In recent years, research on ultra-deep reservoirs in the Kuqa Depression has also advanced significantly. Shou Jianfeng et al. (2003), through studying sandstone diagenesis in the Tarim Basin, were the first to clarify the significant impact of tectonic lateral compression on sandstone compaction. Zhang Ronghu et al. (2014) systematically analyzed the formation mechanism of ultra-deep, low-porosity, tight sandstone reservoirs in the Kelasu Structural Belt, emphasizing the controlling role of tectonic stress on reservoir quality. Zeng Lianbo et al. (2020, 2024) conducted in-depth research on the tectonic alteration effects and fracture distribution patterns in subsalt ultra-deep reservoirs of the Kelasu Structural Belt, proposing models such as fold-controlled fractures and fault-controlled fractures. Previous studies suggest that for every 100 MPa increase in horizontal tectonic stress, sandstone porosity can decrease by an average of 10.51% [12-15].

However, existing theories struggle to fully explain the differences in pore and fracture development between the eastern and western segments, and between different north-south zones within the Kelasu Structural Belt. During the foreland compression process, differences in the stress state of sandstones are key factors influencing primary pore preservation, fracture development, and changes in pore structure. The in-situ stress state varies significantly across different structural positions. When approaching the front of a fold-thrust belt, the near-horizontal component of the stress field parallel to the thrust belt orientation gradually increases, eventually exceeding the vertical component to become the maximum principal stress. Notably, the overall strain degree of the rock does not simply show a positive correlation with the magnitude of in-situ stress; the compressional effect is jointly constrained by factors such as the duration of tectonic stress application and burial depth.

Based on this, this paper selects four typical structures with varying compression intensities—DB16,

DB14, BZ19, and BZ9—in the Bozi-Dabei area of the Kelasu Structural Belt, Kuqa Depression, for detailed analysis. Through sandstone thin-section identification, rock mechanics parameter testing (Young's modulus, Poisson's ratio), rock stress-strain experiments, and in-situ stress measurements, we systematically investigate the stress magnitude and present-day strain state of reservoirs in structural locations with different compression intensities. This reveals the control mechanism of stress-strain degree on reservoir quality, elucidates the stress-controlled reservoir mechanism under strong tectonic compression, and ultimately constructs a stress-controlled reservoir geological model based on structural location. This work aims to provide a theoretical foundation for the exploration and development of ultra-deep natural gas in the study area.

1 Geological Setting

The Kuqa Depression is situated in the northern part of the Tarim Basin, bordered by the South Tianshan Mountains to the north and the Baicheng Sag to the south (Figures 1a, 1b). During the Early Cretaceous, the Bashijiqike Formation developed fan-delta to braided river delta systems. The lithology is predominantly fine sandstone, subdivided from top to bottom into the First, Second, and Third Members of the Bashijiqike Formation (Figure 1e). The Kuqa Depression experienced uplift and denudation due to Late Cretaceous tectonic activity, resulting in a regional unconformity. In the western part of the depression, only the relatively thin Second and Third Members are preserved. Above the end-Cretaceous unconformity, the Paleogene gypsum-salt rocks and Neogene sandy conglomerates were successively deposited. Concurrently, the Kuqa Depression underwent N-S tectonic compression, leading to the formation of numerous imbricate thrust structures within the Cretaceous strata beneath the evaporite layer. These imbricate anticlines are also the primary locations for hydrocarbon accumulation in the area (Figures 1c, 1d) [16-19].

Since the Neogene, intense compression from the South Tianshan Mountains towards the south led to the development of numerous approximately E-W trending folds and thrust faults within the Kuqa foreland basin. Controlled by this N-S compression, multiple rows of imbricate thrust structures and a small number of pop-up structures formed within the Cretaceous strata beneath the evaporite layer. This study selected a typical profile

from the central part of the Bozi-Dabei area: The DB16 block is located in the hanging wall of the Bozi-Kela Fault, characterized by a broad, gentle anticline with shallow burial depth (3500-4000 m) and low confining pressure. The DB14 block is situated in the footwall of the Bozi-Kela Fault and the hanging wall of the Keshen Fault. The BZ1 and BZ19 blocks are located in the proximal part of the footwall of the Kelasu Fault. They are classified as pop-up and pop-down structures with shallow burial depth and low vertical stress. The BZ9 block is located in the distal part of the footwall of the Kelasu Fault and is characterized by an imbricate thrust structure with great burial depth (7700-8000 m).

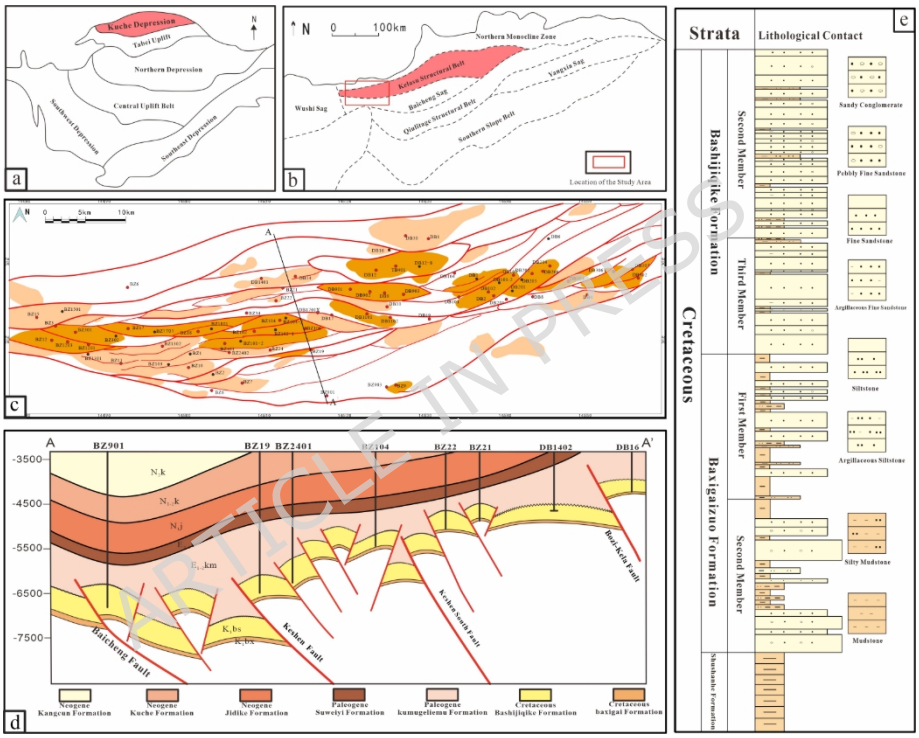

Figure 1 (a, b) Structural unit division of the Kelasu Structural Belt, Kuqa Depression; (c) stratigraphic column of the Cretaceous Bashijiqike Formation; (d) location map of the study area; and (e) stratigraphic profile

2. Pore and Petrophysical Characteristics of Ultra-Deep Tight Sandstones

2.1 Petrology and Pore Characteristics

Based on core observations and casting thin-section analysis, the main rock types are feldspathic lithic sandstone and lithic feldspathic sandstone. The quartz content ranges from 42% to 58%, averaging 48.4%. The feldspar content is relatively low, ranging from 27% to 40%

(avg. 32.5%), predominantly potassium feldspar. The lithic fragment content varies between 7% and 27%, with an average of 15.3%. The detrital grains are medium to fine-grained and vary in size, containing minor siltstone and coarse sandstone. Sorting is moderate to poor, with grain contacts primarily being point-to-line. Roundness is mainly subangular to subrounded, indicating low textural maturity. The main cement type in the northern part of the reservoir sandstone is calcite, while dolomite cementation dominates in the southern part. Siliceous, albite, analcime, and gypsiferous cements are rarely observed.

In the target interval, pore types are dominated by primary intergranular pores and intergranular dissolution pores, with minor intragranular dissolution pores, micro-fractures, and micro-pores (Figure 2a). Primary pores are mainly residual intergranular pores (Figure 2b). Their formation is influenced by various factors such as compaction, resulting in irregular pore shapes. These pores constitute the most important pore type in the target zone. Secondary pores include intergranular and intragranular dissolution pores (e.g., feldspar dissolution pores, lithic fragment dissolution pores). Most intergranular dissolution pores are feldspar dissolution pores, primarily exhibiting banded shapes. Micro-fractures are predominantly tectonic fractures (Figure 2c), mainly appearing as bands cutting across grains, with a small number of contraction fractures. Throat types are mainly linear, tubular, sheet-like, or curved sheet-like, with fine throat sizes. A small number of constricted throats are also present (Figures 2d, 2e, 2f). Scanning Electron Microscope (SEM) observations show that throat sizes vary. Most throats are distributed along grain edges, with radii ranging from 1 to 6 μm. A small number of throats are located at the edges of dissolution pores, also with radii between 1 and 6 μm (Figures 2g, 2h, 2i).

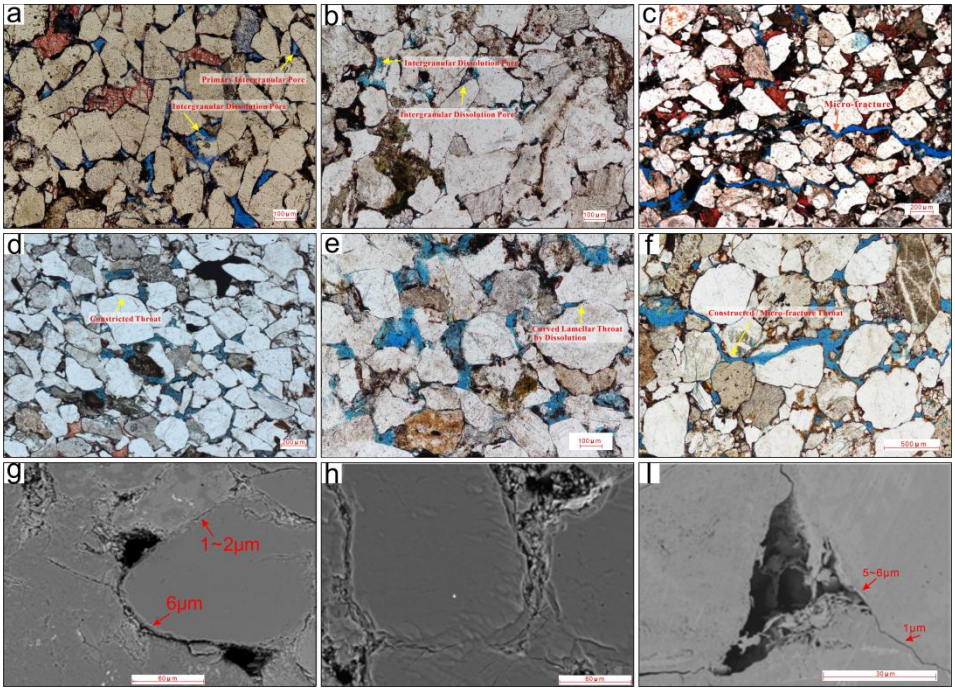

Figure 2 Development characteristics of pores and throats in the Cretaceous Bashijiqike Formation from typical structural gas reservoirs, Bozi-Dabei area

(a) Primary intergranular pores and intergranular dissolution pores, bz19-1, 7699.9 m; (b) Intragranular dissolution pores and intergranular dissolution pores, bz17-1, 6061.3 m; (c) Micro-fractures, bz22-1, 6325 m; (d) Constricted throats, bz24-1, 7219.2 m; (e) Curved lamellar throats by dissolution, bz24-2, 7220.68 m; (f) Constructed and micro-fracture throats, bz22-1, 6325 m; (g) Constricted throat radii of 1–6 μm, bz24-1, 7219.2 m; (h) Curved lamellar throat radii by dissolution of 1–2 μm, bz24-2, 7220.68 m; (i) Curved lamellar throat radii by dissolution of 1–6 μm, bz24-1, 7219.2 m.

The pore distribution in the study area's reservoirs exhibits a characteristic of "segmentation in the east-west direction and zonation in the north-south direction." At the structural belt scale, the content of both primary and secondary pores initially increases and then decreases from north to south and from west to east. On a vertical scale, the content of primary and secondary pores is higher near the unconformity surface.

2.2 Petrophysical Parameter Characteristics

We performed a statistical analysis on petrophysical data from 300 samples across 19 wells in the study area. The results show that the sandstone of the Bashijiqike Formation has a minimum porosity of 1.18%, a maximum porosity of 14.9%, and an average porosity of 6.09%.

Permeability ranges from 0.008×10^{-3} μm² to 230×10^{-3} μm², with an average of 0.3×10^{-3} μm². These values classify it as a low-porosity, low-permeability to tight reservoir (Figure 3). Analysis of cross-plots reveals significant variation in the sandstone's petrophysical properties within the study area. The relationship between porosity and permeability is not simply linear. The presence of micro-fractures in some core samples results in low porosity but relatively high permeability. Overall, the reservoirs can be categorized into pore-type and fracture-type reservoirs. Comparative petrophysical analysis of core samples from key well areas indicates that the DB16 and BZ9 gas reservoirs exhibit a positive correlation between porosity and permeability. These are typical pore-type reservoirs with the best petrophysical properties. The DB14 gas reservoir is also a pore-type reservoir but with somewhat inferior properties. In contrast, the BZ19 and BZ1 reservoirs are fracture-type, showing a weak correlation between porosity and permeability. They generally have lower porosity compared to the DB16 and BZ9 reservoirs.

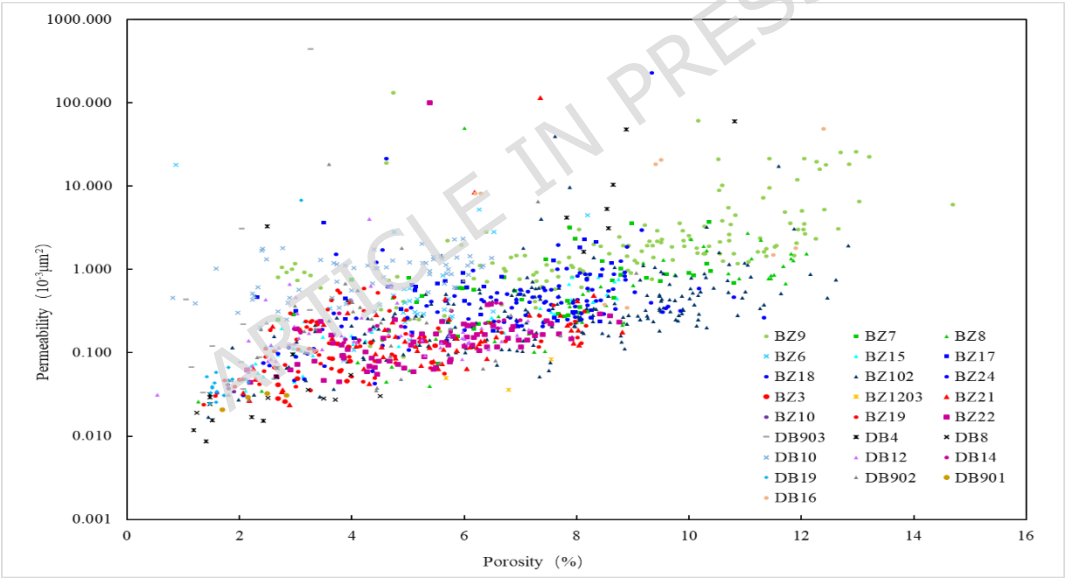

Figure 3 Porosity and permeability characteristics of the Cretaceous Bashijiqike Formation in typical structural gas reservoirs, Bozi-Dabei area

2.3 Diagenesis and Pore Evolution

The ultra-deep Cretaceous reservoirs in the Kelasu Structural Belt of the Kuqa Depression have undergone a complex diagenetic evolution. Compaction is the primary porosity-reducing process, with tensile segments experiencing weaker compaction than compressional segments during tectonic compression and folding deformation. Cementation is predominantly carbonate,

followed by albite and quartz cementation, with minor amounts of gypsiferous and clay mineral cements. Dissolution, mainly of feldspar, lithic fragments, and quartz, is the primary porosity-enhancing process [20-23].

Based on diagenetic mineral assemblages, mineral texture relationships, and integrated with data from fluid inclusions, burial history, thermal history, tectonic evolution history, and pore evolution history, the diagenetic evolution of the Bashijiqike Formation sandstone reservoirs can be divided into two main stages: (1) the Late Cretaceous to Miocene normal burial diagenesis stage, and (2) the Kuqa period and subsequent (5.3–0 Ma) tectonic diagenesis stage. The burial diagenesis stage primarily occurred during the basin depression period, characterized by relative tectonic stability and predominant subsidence. It evolved in the late phase with features transitional to a foreland basin. The tectonic diagenesis stage occurred during the basin's foreland period, a phase of intense crustal shortening and deformation. The intensified convergence of the Eurasian and Indian plates led to strong uplift of the South Tianshan Mountains and the formation of numerous thrust faults and anticlines. During this stage, reservoirs were significantly affected by tectonic compression.

This tectonic diagenesis stage can be further subdivided into four evolutionary periods:Early Cretaceous (127–97 Ma) Slow Burial Compaction and Cementation Period: Characterized by weak compaction, weak siliceous cementation, and strong carbonate cementation. Late Cretaceous (97–65 Ma) Uplift and Epigenetic Leaching/Dissolution Period: Marked by the epigenetic dissolution of carbonate cements and feldspars.Paleogene to End of Miocene (65–5.3 Ma) Re-burial Compaction and Cementation Period: Featured renewed burial compaction, weak gypsum (anhydrite) cementation, and moderate to weak carbonate cementation.Post-Miocene (5.3 Ma–present) Deep Burial and Intense Tectonic Compression Diagenesis Period: Defined by tectonic compaction (porosity reduction and fracture creation) and late-stage acidic fluid dissolution. This period is also the most significant for porosity reduction (Figure 4).

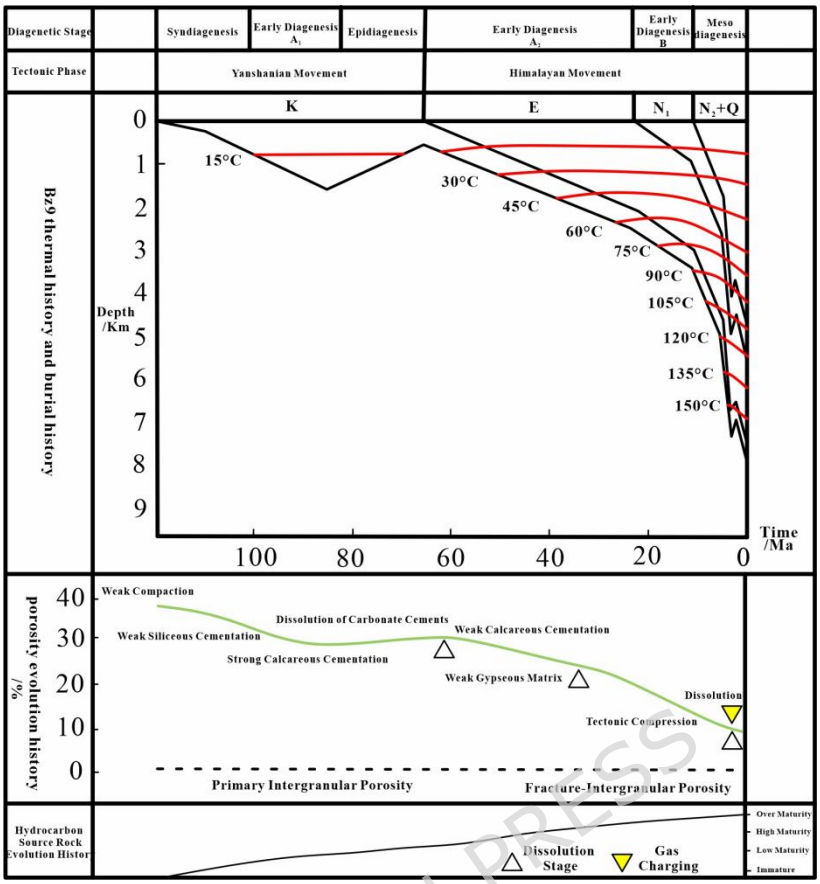

Figure 4 Diagenetic evolution of the Cretaceous Bashijiqike Formation in typical structural gas reservoirs, Bozi-Dabei area

3 Stress-Controlled Reservoir Study

In recent years, with the widespread application of geomechanics in reservoir studies, an increasing number of scholars believe that different stress states exert a significant controlling effect on pore development. The calibration of stress states and the identification of rock strain degree provide important guidance for understanding the development models of deep to ultra-deep reservoirs[23-26]. This study employs an integrated methodology combining experiments, well-logging, and stress simulation to systematically analyze the stress state, strain degree, and petrophysical characteristics of reservoirs in different structural locations within the Kelasu Structural Belt.

3.1 In-situ Stress Measurement and Calculation

The in-situ stress state of a sandstone reservoir, primarily characterized by the maximum horizontal principal stress (σH), minimum horizontal principal stress (σh), and vertical principal stress (σv), reflects its

condition after undergoing deformation from tectonic compression. The two horizontal principal stresses can be determined through rock mechanics experiments. This study systematically calculated the in-situ stress by integrating reservoir characteristics, production test results, previous research findings, and data from rock mechanics and Acoustic Emission (AE) experiments in the study area. For four samples from the same rock core, acoustic emission tests were conducted in the horizontal directions at 0°, 45°, 90°, and in the vertical direction. The paleo-maximum principal stress (the Kaiser effect point) was measured for each of these four orientations.

The paleo-stress under different confining pressures (corresponding to different paleo-vertical stresses at various paleo-burial depths) was determined using the following formula:

$$\sigma_v = \sigma_{Vertical} + \alpha P_P \ldots\ldots\ldots\ldots\ldots\ldots$$

$$\sigma_H = \frac{\sigma_{0^\circ} + \sigma_{90^\circ}}{2} + \frac{\sigma_{0^\circ} - \sigma_{90^\circ}}{2}\left(1 + tg^2 2\theta\right)^{\frac{1}{2}} + \alpha P_p$$

$$\sigma_h = \frac{\sigma_{0^\circ} + \sigma_{90^\circ}}{2} - \frac{\sigma_{0^\circ} - \sigma_{90^\circ}}{2}\left(1 + tg^2 2\theta\right)^{\frac{1}{2}} + \alpha P_p$$

$$tg2\theta = \frac{\sigma_{0^\circ} + \sigma_{90^\circ} - 2\sigma_{45^\circ}}{\sigma_{0^\circ} + \sigma_{90^\circ}}$$

Where:σ_v is the vertical overburden stress;σ_H and σ_h are the maximum and minimum horizontal principal stresses, respectively;Pp is the formation pore pressure; α is the Biot effective stress coefficient (the α in K = f(α, θ) is the angle);$\sigma_{Vertical}$ is the Kaiser point stress measured on the vertically oriented core sample;σ_{0°, σ_{45°, and σ_{90° are the Kaiser point stresses measured on the three horizontally oriented core samples at angles σ_{0°, σ_{45°, and σ_{90°, respectively.

The interpretation method for Acoustic Emission (AE) data under confining pressure is as follows: The stress corresponding to the measured Kaiser effect is subtracted by the vertical principal stress obtained from field well logging data. This calculation yields the variation curve of their difference with changing confining pressure. By then subtracting the regression-derived linear expression from the stress corresponding to the Kaiser effect, the conversion relationship between the Kaiser effect stress under confining pressure and the stress under zero confining pressure is established:

$$\sigma_0 = (\sigma_1 + \sigma_3) - (0.1029\sigma_3 + 1.2293)$$

Where:σ1 is the measured stress corresponding to the Kaiser effect under an applied confining pressure;σ3 is the value of the confining pressure;σ0 is the normal stress in the corresponding direction under zero confining pressure.

As shown in Table 1, the experimental data from the study area indicate that the maximum horizontal principal stress ranges from 151.53 to 203.37 MPa, the minimum horizontal principal stress from 127.46 to 165.22 MPa, and the vertical principal stress from 136 to 194 MPa. The vertical principal stress acts as the intermediate principal stress. Furthermore, the experimental results were used to calibrate the in-situ stress magnitudes interpreted from acoustic well logging data. This calibration enables the extension of continuous in-situ stress profiles across the entire well section, facilitating subsequent analysis of the vertical and lateral variations in stress.

Table 1: Results of Acoustic Emission Experiments for the Bashkiqike Formation in the Bozai-Dabei Area

Sample Set	**ID**	**Confining PressureMPa**	**Depth m**	**Coring Angle**	**Max Horizontal Stress σ_HMPa**	**Min Horizontal Stress σ_hMPa**	**σH Gradient MPa/100m**	**σh Gradient MPa/100m**	**Horizontal Stress Difference MPa**
1	BZ19-0	60	7710	0	203.37	165.22	2.64	2.14	38.15
	BZ19-45	40		45					
	BZ19-90	40		90					
	BZ19-V	60		V					
2	BZ2402-0	40	7210	0	194.73	158.38	2.7	2.2	36.35
	BZ2402-45			45					
	BZ2402-90			90					
	BZ2402-V			V					
3	BZ104-0	40	6856	0	160.45	146.4	2.78	2.22	19
	BZ104-45			45					
	BZ104-90			90					
	BZ104-V			V					
4	DB1604-0	40	5180	0	151.53	127.48	2.74	2.31	24.04
	DB1604-45			45					
	DB1604-90			90					
	DB1604-V			V					

3.2 Differences in In-situ Stress State

Furthermore, experimental results were used to calibrate the in-situ stress magnitudes interpreted from acoustic logging data, enabling extrapolation to obtain a continuous in-situ stress profile for the entire well section and facilitating the analysis of its vertical and lateral variation patterns. In-situ stress simulations were conducted using Abaqus software. The calibrated in-situ stress profiles reveal that the distribution of in-situ stress

in the Kelasu Structural Belt exhibits distinct zonation and stratification characteristics.

The distribution of in-situ stress states is closely related to structural morphology. Within the deformation model of the foreland fold-thrust belt, the study area is characterized by layer-parallel shortening deformation, locally controlled by faults, where variations in structural style lead to changes in the stress difference (Figure 5). The study area is primarily controlled by four faults—the Bozi-Kela Fault, Keshen Fault, South Keshen Fault, and Baicheng Fault—formed by north-south trending tectonic compression resulting from the South Tianshan thrust nappe. From north to south, the area can be divided into four tectonic zones.

The first zone is located south of the South Tianshan Mountains and north of the Bozi-Kela Fault, with the DB16 well area as a representative block. This zone is predominantly characterized by thrust imbricate structures, developing pop-ups and pop-downs, and is generally situated in the hanging wall of the northern structural belt. Due to tectonic uplift, this area has the highest structural position and shallowest burial depth, resulting in relatively low overall in-situ stress values, with maximum horizontal principal stresses ranging between 140-150 MPa.The second zone is situated south of the Bozi-Kela Fault and north of the Keshen Fault, represented by the BZ21 and DB14 well areas. This block is mainly characterized by wide-gentle imbricate structures with minor pop-up structures. Compared to the frontal part of the structure, the central part experiences slightly stronger compression and higher horizontal stress values, with maximum horizontal principal stresses ranging from 150 to 170 MPa.The third zone is located south of the Keshen Fault and north of the South Keshen Fault, with the BZ1 and BZ19 well areas as representatives. This zone is primarily composed of pop-up structures with some imbricate structures, generally positioned in the footwall of the central structural belt. Compared to the structural front, this area has relatively greater burial depth and experiences intense compression, leading to high horizontal stress values. Maximum horizontal principal stresses range from 160 to 180 MPa. Stress values gradually increase from north to south, with stress values within pop-up structures being lower compared to adjacent imbricate structures.The fourth zone lies south of the Baicheng Fault, represented by the BZ9 block. This zone is predominantly characterized by thrust imbricate structures, developing pop-ups and pop-downs. It is

generally located in the footwall of the southern structural belt, experiencing relatively weaker compression, with maximum horizontal principal stresses ranging from 190 to 204 MPa (see Figure 6). Tectonic stress and structural deformation control the intensity of lateral compaction: the higher the tectonic stress in a location, the greater the porosity reduction due to lateral compaction; similarly, locations closer to the core of the anticline (below the neutral surface) exhibit higher porosity reduction from lateral compaction(Table 2).

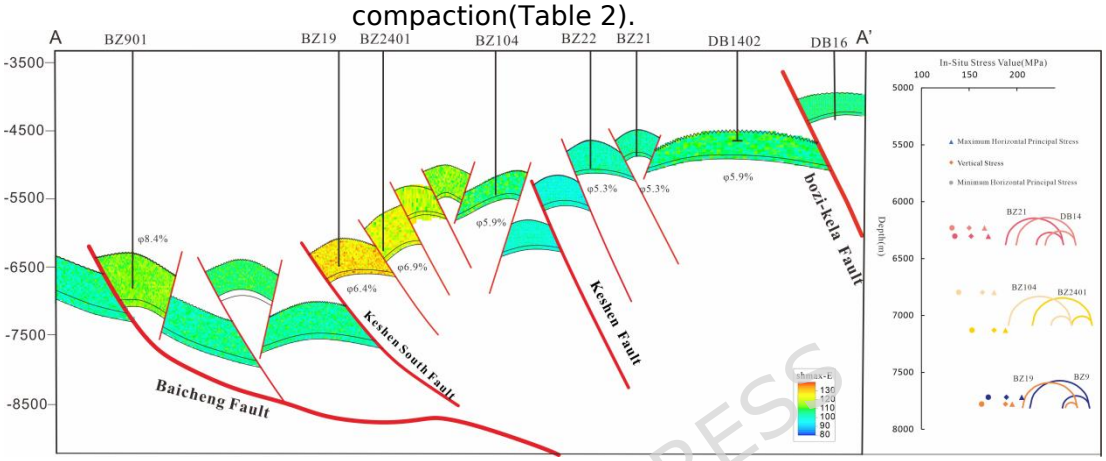

Figure 5 Distribution of the maximum principal stress in the Cretaceous Bashijiqike Formation sandstone across the Kelasu Structural Belt (N-S profile)

Table 2 Regional tectonic and stress characteristics of the Bozi-Dabei area

strip	representative block	tectonic location	tectonic characteristics	stress pattern
1	DB16	North of the Bozi-Kela Fault	Predominantly thrust imbricate structure	Shmax:140-150MPa XY:10-20MPa
2	BZ21,DB14	South of the Bozi-Kela Fault north of the Keshen Fault	Predominantly wide-gentle imbricate structure with minor pop-up structure	Shmax:150-170MPa XY:15-25MPa
3	BZ1□BZ19	South of the Keshen Fault north of the South Keshen Fault	Predominantly pop-up structure with some imbricate structure	Shmax:160-180MPa XY:20-35MPa
4	BZ9	South of the South Keshen Fault north of the Baicheng Fault	Predominantly thrust imbricate structure	Shmax:190-204MPa XY:10-15MPa

3.3 Analysis of Rock Mechanics Parameters

During burial, as depth increases or tectonic compression intensifies, rock density and hardness correspondingly increase, manifested as an increase in Young's modulus and a decrease in Poisson's ratio. Under similar lithological conditions, Young's modulus and Poisson's ratio can approximately reflect the magnitude of paleo-stress the rock has experienced. Notably, the time-integrated stress magnitude (the integral of stress over time) significantly impacts reservoirs, and Young's modulus and Poisson's ratio are the petrophysical parameters that record this information. Based on extensive experimental and well-logging data, this study calculated parameters such as in-situ stress, rock mechanics parameters, and porosity for the four structural zones from north to south within the Kelasu Structural Belt (Figure 6).

Comprehensive analysis indicates that the different north-south zones of the Kelasu Structural Belt exhibit variations in micro-fracture development due to differences in sedimentary fabric and in-situ stress:Zone I features low stress, small stress difference, and moderate compression; coarse rock grain size, high matrix content, and poor sorting; small Young's modulus, large Poisson's ratio, and low fracture density.Zones II and III are characterized by medium stress, large stress difference, and strong compression; fine rock grain size and good sorting; large Young's modulus, small Poisson's ratio, and high resistance to compression, making them prone to fracture formation.Zone IV exhibits high stress, medium stress difference, and weak compression; fine rock grain size and good sorting; relatively large Young's modulus, relatively small Poisson's ratio, and well-developed porosity.

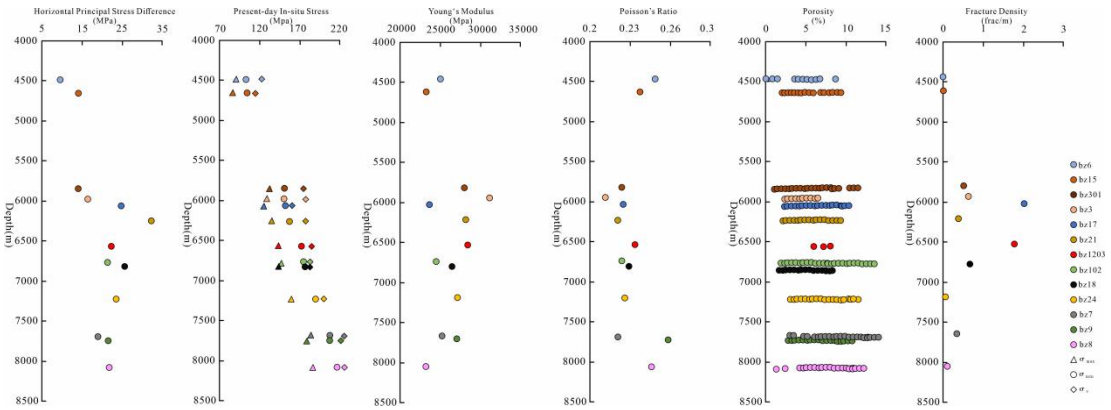

Figure 6 Relationship diagram of in-situ stress, rock mechanics parameters, and porosity across different structural locations in the Kelasu Structural Belt

3.4 Relationship between Rock Mechanics Parameters and Petrophysical Properties

Stress is a complex parameter with both magnitude and direction, varying at different depths and orientations. The measurement and restoration of paleo-stress are extremely difficult. Young's modulus and Poisson's ratio represent a comprehensive manifestation of triaxial and even polyaxial stress states, recording information on burial depth, confining pressure, and tectonic compressive stresses from various directions, particularly the maximum principal stress. Therefore, Young's modulus and Poisson's ratio best reflect the integrated paleo-stress and strain degree of rock at a given subsurface depth.

Analysis of rock mechanical parameters in the study area indicates that Young's modulus is positively correlated with compressive strength and maximum horizontal principal stress (Figures 7a, 7c). Conversely, Young's modulus and maximum horizontal effective principal stress are negatively correlated with porosity (Figures 7b, 7d). This suggests that as the degree of strain increases, the rock becomes more compact, its mechanical strength increases, and porosity decreases.

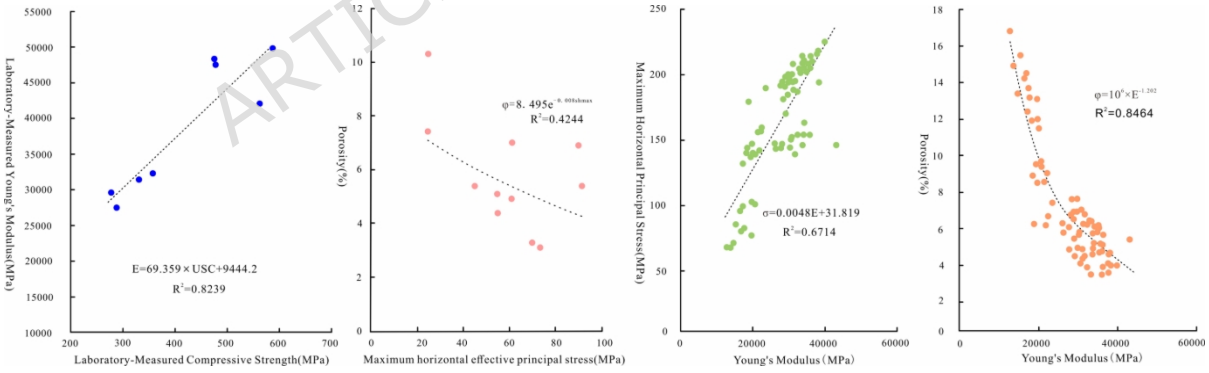

Figure 7 Cross-plots of rock mechanical parameters versus porosity for the reservoir in the Bashijiqike Formation, Kelasu Structural Belt

4 Reservoir-Controlling Model for Ultra-Deep Tight Sandstones

4.1 Strain Degree and Pore-Fracture Evolution Model

Tectonic compression exerts a dual impact on reservoir physical properties: porosity reduction and fracture formation. Previous experimental simulations of

consolidated sandstone under compression have revealed that prolonged compression leads to a gradual decrease in porosity, the progressive formation of more stable grain contact configurations, and a clear linear relationship between rock mechanical parameters and porosity. In deeper strata, as diagenesis intensifies and stress increases, microfractures develop within the rock. A distinct pattern exists between the compressive stress-strain relationship and the degree of porosity reduction and fracture development in the study area, and even across the typical gas reservoirs of the entire Bozi-Dabei area (Figure 8).The cross-plot of Young's modulus versus Poisson's ratio identifies three distinct stages for reservoirs in this area. The first stage represents the initial phase of stress accumulation. Pore types are primarily primary intergranular pores. Young's modulus ranges from 18,000 to 25,000 MPa, Poisson's ratio ranges from 0.25 to 0.3, and porosity ranges from 6% to 10%. The second stage corresponds to the stress concentration to initial stress release phase. Pore types are still dominated by primary intergranular pores, with a small number of microfractures. Young's modulus ranges from 25,000 to 40,000 MPa, Poisson's ratio ranges from 0.22 to 0.25, and porosity ranges from 4% to 6%. However, due to the formation of micro- to macro-fractures in some samples, permeability increases. The third stage is the stress release phase. Microfractures are relatively well-developed within the pores. The macroscopic linear fracture density in the reservoir ranges from 0.2 to 0.3. Young's modulus ranges from 30,000 to 36,000 MPa, Poisson's ratio ranges from 0.17 to 0.22, and porosity ranges from 4% to 6%. Overall, the Bozi area has experienced a higher degree of compression compared to the Dabei area, resulting in denser rock, a higher degree of fracture development, and lower porosity.

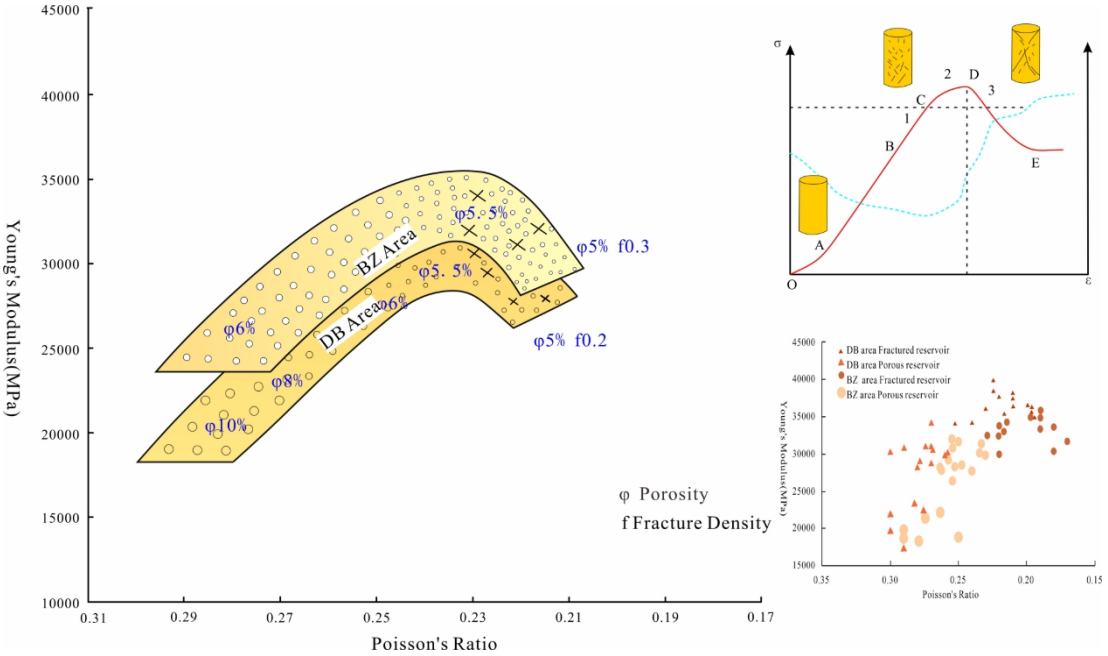

Figure 8 Cross-plot of Poisson's ratio versus Young's modulus for the Cretaceous Bashijiqike Formation reservoirs in typical structural gas reservoirs, Kelasu Structural Belt

4.2 Stress-Controlled Reservoir Models in Different Structural Zones

Based on the relationship between maximum horizontal principal stress and physical properties, the stress profile can be converted into a physical property profile. Combined with an analysis of strain degree differences, the strain characteristics and pore-fracture evolution models for different structural positions in the hanging wall and footwall of faults within the Kelasu Structural Belt can be established (Figure 9). From north to south, the area can be divided into four tectonic zones:The proximal footwall structure of the Kelasu Fault (e.g., the DB16 area), due to the uplifting effect of hanging wall thrusting, experiences low vertical stress, forming a pop-down structure with weak compression. This results in good physical properties, with porosity reaching up to 10% and underdeveloped fractures (density < 0.2).The central footwall area (e.g., BZ19) exhibits high stress with localized stress concentration, corresponding to the strongest effective compressional stress. This forms strongly compressed imbricate structures and pop-up imbricate structures, leading to a high degree of strain, porosity below 5%, and well-developed fractures (density > 0.3, up to 0.8).The distal footwall area (e.g., BZ9) is characterized by high

stress values but a small stress difference, resulting in the weakest effective compressional stress. This forms wide-gentle pop-up imbricate structures with a low degree of strain, porosity exceeding 9%, and underdeveloped fractures (density < 0.2).

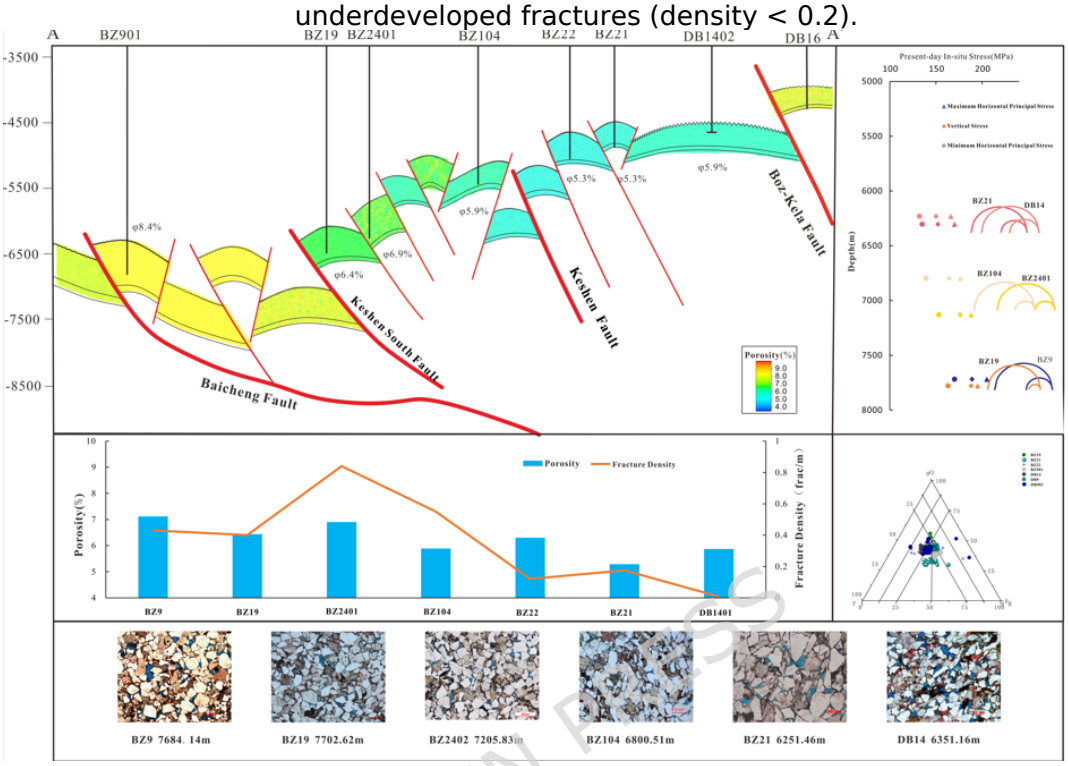

Figure 9 A Model Diagram of Stress-Strain and Porosity-Permeability Evolution for Cretaceous Bashijiqike Formation Reservoirs in Typical Structural Gas Reservoirs, Kelasu Structural Belt

This understanding reveals how variations in stress magnitude and strain degree at typical structural positions within the Kelasu Structural Belt control reservoir quality. It provides a reliable geological basis for reservoir prediction in the next phase of natural gas exploration and development in this region.

5 Conclusions

(1) In the Bozi-Dabei area of the Kelasu Structural Belt, the porosity of the Bashijiqike Formation sandstone ranges from 1.18% to 14%, with an average of approximately 6.5%. Permeability ranges from (0.008 to 230) × 10^{-3} μm², with an average of 0.3 × 10^{-3} μm², classifying it as a low-porosity, ultra-low-permeability to tight reservoir. Pore types are primarily primary intergranular pores and intergranular dissolution pores, with minor intragranular dissolution pores, microfractures, and micropores. The reservoir is significantly influenced by tectonic compression. The

diagenetic evolution comprises four stages, with the most critical being the deep burial and strong tectonic compression stage since the end of the Miocene. This stage is characterized by tectonic compaction-induced porosity reduction and fracture formation, along with late-stage acidic fluid dissolution, and represents the most important period of porosity loss.

(2) Integrating acoustic emission experimental data with well log interpretations, four distinct tectonic belts have been identified along a north-south cross-section. From north to south, the maximum horizontal principal stress and horizontal stress difference first increase and then decrease. The central tectonic belt, subjected to intense compression, exhibits pop-up structures. The flanking belts, experiencing weaker compression, display thrust imbricate structures, with the southern belt showing the weakest compressional effects.

(3) A quantitative evaluation method for strain degree based on rock mechanical parameters has been established. By analyzing the relationship between rock mechanical parameters and physical properties, the correlation between rock strain degree and reservoir properties was established in the study area. Three types of pore-throat assemblages were identified, whose characteristics can clearly distinguish high-strain fractured reservoirs from low-strain porous reservoirs. This provides a new approach for predicting reservoir types using conventional well log data.

(4) The "stress-strain" controlled reservoir model elucidated in this study indicates that strong compressional stress significantly modifies reservoir porosity and permeability through fracture generation. The established model provides an important theoretical basis and practical guidance for predicting favorable reservoirs and optimizing drilling targets in different structural positions within the Kelasu Structural Belt.

Acknowledgment

We would like to give our gratitude to CNPC Tarim oil field for providing the test samples and their inputs on parts of the experimental data

Funding

"Fine Characterization and Evaluation Technology for Deep-Ultra Deep Clastic Traps" (2025ZD1402401) from CNPC Tarim Oilfield

Data Availability Statement

The raw data supporting the conclusions of this article will be made available by the authors on request.

References:

[1] Guo, X., Hu, Z., Li, S., et al. Research progress and prospect of deep and ultra-deep natural gas exploration. Petroleum Science Bulletin.2023, 8(4), 461–474.

[2] Cao, Y., Yuan, G., Yang, H., et al.. Current status of oil and gas exploration in deep-ultra deep clastic rocks of petroliferous basins and research progress on the genesis of high-quality reservoirs. Acta Petrolei Sinica .2022, 43(1), 1–18.

[3] Li, Z.. Diagenetic dynamics in deep and ultra-deep parts of sedimentary basins: Some research advances and specific problems. Acta Sedimentologica Sinica.2023, 41(6)

[4] Liu, C., Zhang, H., Han, B., et al. Characteristics and controlling factors of deep clastic reservoir in Dabei area, Kuqa Depression. Natural Gas Geoscience.2009, 20(4), 504-512.

[5] Wang, C., Li, H., Chen, D., et al. Pore structure characteristics and influencing factors of tight sandstone reservoirs in Bashijiqike Formation of Keshen Gasfield. Geological Science and Technology Information. 2018, 37(5), 70-77.

[6] Han, D., Li, Z., Han, Y., et al. The closeness of burial diagenetic environment and differentiation of cementation for Cretaceous sandstone in Kelasu thrust belt of Kuqa Depression. Acta Petrologica Sinica. 2009, 25(10), 2351-2362.

[7] Zhang, R., Zhang, H., Shou, J., Shen, Y., & Li, C. Geological analysis on reservoir genesis of Lower Cretaceous Bashijiqike Formation in Dabei area, Kuqa Depression. Chinese Journal of Geology.2008, 43(3), 507-517.

[8] Warren E A, Pulham A J. Anomalous porosity and permeability preservation in deeply buried Tertiary and Mesozoic sandstones in the Cusiana field, Llanos Foothills, Colombia[J]. Journal of Sedimentary Research, 2001, 71(1): 2-14.

[9] Potocki D, Hutcheon I. Lithology and Diagenesis of Sandstones in the Western Canada Foreland Basin: Chapter 8[J]. 1992.

[10] Monsees A C, Busch B, Schöner N, et al. Rock typing of diagenetically induced heterogeneities–A case study from a deeply-buried clastic Rotliegend reservoir of the Northern German Basin[J]. Marine and Petroleum Geology, 2020, 113: 104163.

[11] Laczkó-Dobos E, Gier S, Sztanó O, et al. Porosity development controlled by deep-burial diagenetic process in lacustrine sandstones deposited in a back-arc basin (Makó Trough, Pannonian Basin, Hungary)[J]. Geofluids, 2020, 2020: 1-26.

[12] Zhang, H., Zhang, R., Yang, H., et al. Quantitative evaluation method and application for sandstone reservoir with developed structural fractures: A case study of Cretaceous in Kuqa foreland basin. Acta Petrologica Sinica.2012, 28(3), 827-835.

[13] Zhang, H., Zhang, R., Yang, H., et al. Characterization and evaluation of ultra-deep fractured-pore tight sandstone reservoirs: A case study of Cretaceous Bashijiqike Formation in Kelasu tectonic zone, Kuqa foreland basin. Petroleum Exploration and Development.2014, 41(2), 158-167.

[14] Pan, R., Zhu, X., Liu, F., Li, Y., & Zhang, J. Diagenesis of Cretaceous reservoirs in Kelasu thrust belt and its influence on reservoir quality. Acta Sedimentologica Sinica. 2014, 32(5), 973-980.

[15] Wang, K., Zhang, R., Zeng, Q., et al. Characteristics and genetic mechanism of deep to ultra-deep reservoirs of Lower Cretaceous in Bozi-Dabei area, Kuqa Depression. Journal of

China University of Mining & Technology. 2022, 51(2), 311-328.
[16] Jiang, X., Shi, L., Mo, T., et al. Characteristics and origin of physical property differences in deep-ultra deep tight sandstone reservoirs: A case study of Bashijiqike Formation in Bozi area, Kuqa Depression. Geological Science and Technology Bulletin.2024.
[17] Pan, R., Zhu, X., Liu, F., et al. Diagenesis of Cretaceous reservoirs in Kelasu thrust belt and its influence on reservoir quality. Acta Sedimentologica Sinica.2014, 32(5), 973-980.
[18] Wang, K., Zhang, R., Wang, J., et al. Distribution characteristics and genesis of structural fractures in ultra-deep tight sandstone reservoirs: A case study of Keshen Gasfield, Kuqa foreland thrust belt, Tarim Basin. Oil & Gas Geology. 2021, 42(2), 338-353.
[19] Wang, Z., Wang, C., Xu, K., et al. Development characteristics and controlling factors of structural fractures in ultra-deep tight sandstone: A case study of Lower Cretaceous reservoirs in Bozi-Dabei area, Kuqa Depression, Tarim Basin. Natural Gas Geoscience. 2023, 34(9), 1535-1551.
[20] Mao, Y. Pore evolution model of Lower Cretaceous sandstone reservoirs in the foreland thrust belt of the Kuqa Depression [Doctoral dissertation, China University of Petroleum (Beijing)]. 2019.
[21] Sun, H., Zhong, D., Li, Y., et al. Pore genesis and controlling factors of ultra-deep, low-porosity, and extra-low permeability sandstone reservoirs: A case study from the Bashijiqike Formation in the Keshen area, Kuqa Depression. Journal of Jilin University (Earth Science Edition). 2018, 48(3), 1–18.
[22] Han, Z., Zeng, L., Gong, L., Zhu, R., & Gao, Z. Differential subsidence of different structural zones in the Kuqa Depression and its influence on reservoir porosity. Chinese Journal of Geology. 2014, 49(1), 104-113.
[23] Warren E A, Pulham A J. Anomalous porosity and permeability preservation in deeply buried Tertiary and Mesozoic sandstones in the Cusiana field, Llanos Foothills, Colombia[J]. Journal of Sedimentary Research, 2001, 71(1): 2-14.
[24] Potocki D, Hutcheon I. Lithology and Diagenesis of Sandstones in the Western Canada Foreland Basin: Chapter 8[J]. 1992.
[25] Monsees A C, Busch B, Schöner N, et al. Rock typing of diagenetically induced heterogeneities–A case study from a deeply-buried clastic Rotliegend reservoir of the Northern German Basin[J]. Marine and Petroleum Geology, 2020, 113: 104163.
[26] Laczkó-Dobos E, Gier S, Sztanó O, et al. Porosity development controlled by deep-burial diagenetic process in lacustrine sandstones deposited in a back-arc basin (Makó Trough, Pannonian Basin, Hungary)[J]. Geofluids, 2020, 2020: 1-26.